$Mn[OPR_2O]_2$. All of the manganese(II) phosphinates in this study are pure white with subnormal magnetic moments. The properties of $Mn[OP(C_4H_9)_2O]_2$ are almost identical with those of $Mn[OP(C_8H_{17})_2O]_2$, including the presence of three strong PO_2 stretching bands in its infrared spectrum.[6] In contrast, there are only two strong PO_2 stretching bands in the spectra of both $Mn\{OP[CH(CH_3)CH_2CH_2CH_3]_2O\}_2$ and $Mn\{OP[C(CH_3)_3]_2O\}_2$, and the separation of these bands is consistent with symmetrical phosphinate groups. The molecular weight of $Mn\{OP[CH(CH_3)CH_2CH_2CH_3]_2O\}_2$ in carbon tetrachloride is greater than 35000, whereas $Mn\{OP[C(CH_3)_3]_2O\}_2$ is insoluble in all solvents tested. Its x-ray powder pattern shows $Mn\{OP[C(CH_3)_3]O\}_2$ to be isomorphous with the *tert*-butylphosphinates of cobalt(II), zinc(II), and nickel(II), and therefore it should also have a distorted tetrahedral structure. It is generally believed that tetrahedrally coordinated manganese(II) compounds are yellow or green and those with octahedral symmetry are white. The white appearance of $Mn\{OP[C(CH_3)_3]_2O\}$ must then be rationalized on the basis that it does not have pure tetrahedral symmetry and therefore p–d orbital mixing cannot occur.

$Cu[OPR_2O]_2$. The properties of $Cu[OP(C_4H_9)_2O]_2$ are similar to those of $Cu[OP(C_8H_{17})_2O]_2$, suggesting that the same type of structure occurs in both materials.[6] On the other hand, $Cu\{OP[C(CH_3)_3]_2O\}_2$ is insoluble in all solvents tested and isomorphous with all of the other *tert*-butylphosphinates in this study. Thus, $Cu\{OP[C(CH_3)_3]_2O\}_2$ should also have distorted tetrahedrally coordinated metal centers and symmetrical bridging phosphinate groups.

Conclusions

It is evident from this study that the first-row transition metal(II) bis(phosphinates) with bulky side groups prefer a configuration with tetrahedrally coordinated metal centers and bridging phosphinate groups, whereas for those with linear-chain alkyl side groups other configurations readily occur. Although the length of the alkyl chain side groups has little effect on the structure of the bis(phosphinates), some physical property differences are observed for different chain lengths. The magnetic behavior of these and other phosphinate polymers is presently being investigated,[16] but to date it has not been possible to correlate the structural parameters with the magnetic properties in these simple metal(II) systems.

Acknowledgment. The authors wish to thank Dr. Campbell Scott of the University of Pennsylvania for making the magnetic measurements on the Faraday balance. They are also grateful to Drs. Piero Nannelli and B. P. Block for helpful discussions. This work was supported in part by the Office of Naval Research and the Advance Research Projects Agency.

Registry No. $Zn[OP(C_4H_9)_2O]_2$, 29469-35-0; $Zn[OP(CH(CH_3)CH_2CH_2CH_3)_2O]_2$, 58281-30-4; $Zn[OP(C(CH_3)_3)_2O]_2$, 58281-32-6; $Co[OP(C_4H_9)_2O]_2$, 36788-28-0; $Co[OP(CH(CH_3)CH_2CH_2CH_3)_2O]_2$, 58281-34-8; $Co[OP(C(CH_3)_3)_2O]_2$, 56698-21-6; $Cu[OP(C_4H_9)_2O]_2$, 58281-36-0; $Cu[OP(C(CH_3)_3)_2O]_2$, 58281-38-2; $Mn[OP(C_4H_9)_2O]_2$, 52664-86-5; $Mn[OP(CH(CH_3)CH_2CH_2CH_3)_2O]_2$, 58281-40-6; $Mn[OP(C(CH_3)_3)_2O]_2$, 56698-23-8; $Ni[OP(C_4H_9)_2O]_2$, 58281-42-8; $Ni[OP(C(CH_3)_3)_2O]_2$, 58281-44-0.

References and Notes

(1) Part XVIII: P. Nannelli, H. D. Gillman, and B. P. Block, *J. Polym. Sci., Polym. Chem. Ed.*, **13**, 2849 (1975). In these polymer compositions the substituents on the phosphorus are known as side groups, a terminology commonly used in polymer chemistry to denote groups attached to the polymer backbone.
(2) B. P. Block, *Inorg. Macromol. Rev.*, **1**, 115 (1970).
(3) F. Giordano, L. Randaccio, and A. Ripamonti, *Acta Crystallogr., Sect. B*, **25**, 1057 (1969), and references cited therein.
(4) J. J. Pitts, M. A. Robinson, and S. I. Trotz, *J. Inorg. Nucl. Chem.*, **30**, 1299 (1968).
(5) (a) E. I. Matrosov and B. Fisher, *Izv. Akad. Nauk SSSR, Neorg. Mater.*, **3**, 545 (1967); (b) V. V. Korshak, A. M. Polyakova, O. V. Vinogradova, K. N. Anisimov, N. E. Kolobova, and M. N. Kotova, *Izv. Akad. Nauk SSSR, Ser. Khim.*, 642 (1968).
(6) H. D. Gillman, *Inorg. Chem.*, **13**, 1921 (1974).
(7) G. M. Kosolapoff, *J. Am. Chem. Soc.*, **71**, 369 (1949).
(8) The formula $[OP(C_4H_9)_2O]$ is used exclusively for $[OP(CH_2CH_2CH_2CH_3)_2O]$ in this work.
(9) S. H. Rose and B. P. Block, *J. Am. Chem. Soc.*, **87**, 2076 (1965).
(10) V. Giancotti, F. Giordano, and A. Ripamonti, *Makromol. Chem.*, **154**, 271 (1972).
(11) V. Giancotti and A. Ripamonti, *Chim. Ind. (Milan)*, **48**, 1065 (1966).
(12) S. V. Vinogradova, V. V. Korshak, O. V. Vinogradova, A. M. Polyakova, K. N. Anisimov, and N. Ye. Kolobova, *Vysokomol. Soedin., Ser. A*, **15**, 581 (1973).
(13) W. C. Drinkard and G. M. Kosolapoff, *J. Am. Chem. Soc.*, **74**, 5520 (1952).
(14) H. D. Gillman, *Inorg. Chem.*, **11**, 3124 (1972).
(15) S. H. Rose and B. P. Block, *J. Polym. Sci., Part A-1*, **4**, 573 (1966).
(16) J. C. Scott, A. F. Garito, A. J. Heeger, P. Nannelli, and H. D. Gillman, *Phys. Rev. B*, **12**, 356 (1975).

Contribution from Rocketdyne,
a Division of Rockwell International, Canoga Park, California 91304

trans-Dihydridotetrafluorophosphate(V) Anion, *trans*-$H_2PF_4^-$

KARL O. CHRISTE,* CARL J. SCHACK, and E. C. CURTIS

Received September 3, 1975 AIC50654A

The novel $H_2PF_4^-$ anion was synthesized in the form of its K^+ and Cs^+ salts. Both compounds are white stable solids decomposing at 266 and 284 °C, respectively. Vibrational and ^{19}F NMR spectroscopy show that the anion has a pseudooctahedral structure with the hydrogen ligands in trans position. All ten active fundamentals expected for symmetry D_{4h} were observed and assigned. A normal-coordinate analysis was carried out and shows that $H_2PF_4^-$ contains highly polar PF bonds.

Introduction

During the synthesis of H_2PF_3 according to the method[1] of Holmes and Storey we observed that the NaF, used for the removal of the HF impurity, formed a labile adduct with H_2PF_3. Whereas numerous alkyl- or aryl-substituted fluorophosphates are known,[2,3] to our knowledge no reports have been published on the existence of the corresponding parent compounds, the hydridofluorophosphates. In view of this and the general interest in fluorine-substituted phosphorus compounds, it seemed interesting to synthesize stable hydridofluorophosphates. For $H_2PF_4^-$ further interest was added by the question of whether the two hydrogen ligands are in cis or in trans position.

Experimental Section

Apparatus and Materials. The materials used in this work were manipulated in a well-passivated (with ClF_3) 304 stainless steel vacuum line equipped with Teflon FEP U-traps and 316 stainless steel bellows-seal valves (Hoke, Inc., 4251 F4Y). Pressures were measured with a Heise Bourdon tube type gauge (0–1500 mm ±0.1%). Because of the rapid hydrolytic interaction with moisture, all materials were

handled outside of the vacuum system in the dry nitrogen atmosphere of a glovebox.

The infrared spectra were recorded on a Perkin-Elmer Model 457 spectrophotometer. The spectra of solids at room temperature were obtained by pressing two small single-crystal platelets of either AgCl or AgBr to a disk in a Wilks minipellet press. The powdered sample was placed between the platelets before starting the pressing operation. The instrument was calibrated by comparison with standard calibration points.[4]

The Raman spectra were recorded on a Cary Model 83 spectrophotometer using the 4880-Å exciting line and a Claassen filter[5] for the elimination of plasma lines. For low-temperature work a Miller Harney device[6] was used. Glass or Teflon FEP capillaries were used as sample tubes in the transverse-viewing, transverse-excitation technique. Polarization measurements were carried out according to method VIII listed by Claassen et al.[5]

The ^{19}F NMR spectra were recorded at 56.4 MHz on a Varian high-resolution NMR spectrometer equipped with a variable-temperature probe. Chemical shifts were determined by the side-band technique with an accuracy of ±1 ppm relative to the external standard $CFCl_3$. Teflon FEP liners (Wilmad Glas Co.,) inserted into glass NMR tubes were used as sample containers and CH_3SOCH_3 was used as a solvent.

Debye–Scherrer powder patterns were taken using a GE Model XRD-6 diffractometer with copper Kα radiation and a nickel filter. Samples were sealed in quartz capillaries (~0.5-mm o.d.).

A Perkin-Elmer differential scanning calorimeter, Model DSC-1B, was used for the determination of the thermal stability of the compounds. The samples were crimp-sealed in aluminum pans, and heating rates of 10°/min were used.

Cesium fluoride and KF were fused in a platinum crucible and powdered in a drybox prior to use. The H_2PF_3 was prepared and purified as previously described.[1]

Synthesis of CsH_2PF_4 and KH_2PF_4. Dry KF (2.27, mmol) was placed into a 10-ml stainless steel cylinder and H_2PF_3 (3.13 mmol) was added at −196 °C. The cylinder was kept at −20 °C for 2 days. Excess H_2PF_3 was removed from the cylinder by pumping for several hours at room temperature. Based on the weight gain of the solid 2.19 mmol of H_2PF_3 was complexed. This corresponded to a 96.5% conversion of the KF to KH_2PF_4. The product was a white powder. Anal. Calcd for KH_2PF_4: K, 26.4; P, 20.9. Found: K, 26.7; P, 20.5.

Similarly, CsF (2.51 mmol) when combined with H_2PF_3 (3.21 mmol) at −20 °C resulted in the uptake of 2.51 mmol of H_2PF_3 corresponding to a 100% conversion of the CsF to CsH_2PF_4. The solid product was slightly off-white. The same results were obtained on combining these materials at room temperature, but the product had a light brown color. Anal. Calcd for CsH_2PF_4: Cs, 54.9; P, 12.8. Found: Cs, 55.0; P, 12.6.

The NaF–H_2PF_3 System. Sodium fluoride also interacted with excess H_2PF_3 at −20 °C although the conversion of NaF to NaH_2PF_4 was considerably lower than that observed for KF and CsF. After 10 days at −20 °C only 35% of the NaF had been converted to NaH_2PF_4. The solid product slowly evolved H_2PF_3 on standing at ambient temperature.

Results and Discussion

Syntheses and Properties. Alkali metal fluorides interact with H_2PF_3 with adduct formation. Whereas NaF forms an adduct unstable at room temperature, both KF and CsF form with excess H_2PF_3 at −20 °C 1:1 adducts in quantitative yield. Both KH_2PF_4 and CsH_2PF_4 are white hygroscopic solids, stable at room temperature and according to DSC data undergo exothermic decomposition at 266 and 284 °C, respectively. Since simple dissociation of the adducts to alkali metal fluorides and H_2PF_3 should be endothermic, the DSC results suggested that the thermal decomposition of these salts involved HF elimination and was probably accompanied by alkali metal bifluoride formation. This was experimentally confirmed when CsH_2PF_4 was subjected to careful vacuum pyrolysis. The volatile decomposition products were trapped at −196 °C and after warm-up to room temperature consisted of HF, PF_3, H_2PF_3, and a pale yellow to orange nonvolatile solid. This solid was extremely reactive and pyrophoric, and upon hydrolysis a gas was evolved exhibiting the characteristic smell of phosphine. A full characterization of this solid was beyond the scope of the present study, but the observed properties strongly suggest an associated species containing PP bonds. The $H_2PF_4^-$ salts are highly soluble in CH_3SOCH_3 and moderately soluble in CH_3CN. Attempts to obtain their x-ray powder diffraction patterns in quartz capillaries were unsuccessful owing to chemical attack of the capillaries. The only patterns observable were those of the corresponding SiF_6^{2-} salts.

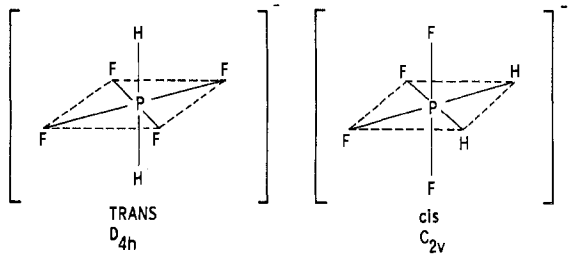

Figure 1. Two possible structural models of $H_2PF_4^-$.

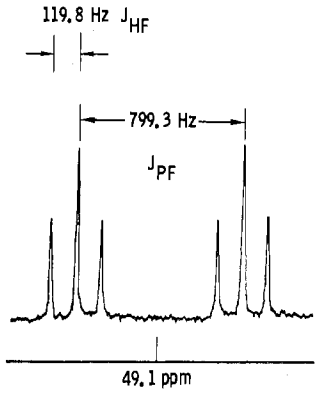

Figure 2. ^{19}F NMR spectrum of $K^+H_2PF_4^-$ in CH_3SOCH_3 solution.

The relatively high thermal stability of these $H_2PF_4^-$ salts and their relative ease of formation are surprising in view of previous reports.[2] Thus, CsF did not form adducts with dialkyltrifluorophosphoranes and the $(CH_3)_2PF_4^-$ anion could only be prepared from $(CH_3)_2PF_3$ and $(CH_3)_3SiN{=}PR_3$. The stability of the resulting salt was attributed to the stabilizing effect of the bulky and resonance-stabilized $[(CH_3)_2P(N{=}PR_3)_2]^+$ cation.

Possible Structures of $H_2PF_4^-$. The hydrogen ligands in $H_2PF_4^-$ could be in either cis or trans position. A priori, it is difficult to predict which of the two isomers is more likely. Whereas in $(CH_3)_2PF_4^-$ and $(CF_3)_2PF_4^-$ the two methyl ligands are trans,[2,3] the oxygen ligands in $IO_2F_4^-$ [7,8] and $TeO_2F_4^{2-}$ [9-11] are cis. For $TeF_4(OH)_2^-$, [11,12] $TeF_4(OCH_3)_2$,[9,13] and $TaF_4Cl_2^-$ [14] both the cis and the trans isomer were observed.

As can be seen from Figure 1, the trans isomer of $H_2PF_4^-$ has higher symmetry than the cis isomer, and therefore, NMR and vibrational spectroscopy should readily distinguish between these two stereoisomers.

^{19}F NMR Spectra. The ^{19}F NMR spectra of KH_2PF_4 and CsH_2PF_4 in CH_3SOCH_3 solution were recorded. They consisted of a well-resolved doublet of triplets (see Figure 2). The observed chemical shifts and coupling constants are listed in Table I.

The trans isomer contains four equivalent fluorine and two equivalent hydrogen atoms. Therefore, the ^{19}F resonance should consist of a doublet of triplets owing to P–F and H–F spin–spin coupling, respectively. For the cis isomer two doublets of triplets would be expected owing to the presence of two nonequivalent pairs of fluorines. The observed spectrum

Table I. ^{19}F NMR Spectral Data for $H_2PF_4^-$ in CH_3SOCH_3 Solution Compared to Those of Related Phosphorus Fluorides

Compd	δ, ppm	J_{PF}, Hz	J_{HF}, Hz
KH_2PF_4	49.1	799.3	119.8
CsH_2PF_4	47.6	798.7	120.8
PF_6^- [a]	73	715	
$(CH_3)_2PF_4^-$ [a]	20.9	856	
HPF_4 [b]	49.6	892	(91)[c]
H_2PF_3 [b]	48.0	860	(80)[c]

[a] Data from ref 2. [b] Data from ref 1; the δ values are the average of rapidly exchanging equatorial and axial fluorines. [c] These values were taken from the proton spectrum; they were not observed in the ^{19}F spectrum owing to the great line width of the signals caused by the rapid exchange of the equatorial and axial fluorine ligands.

agrees with the predictions for the trans isomer and the observed chemical shift and coupling constants agree well with those[1,2] of the related phosphorus fluorides listed in Table I.

Vibrational Spectra. The vibrational spectra of KH_2PF_4 and CsH_2PF_4 provide additional proof for $H_2PF_4^-$ possessing the trans configuration. The observed spectra are shown in Figure 3. The Raman spectra of CsH_2PF_4 were also recorded but are not shown in the figure owing to their similarity to those of KH_2PF_4. The observed frequencies are listed in Table II. Although no laser-induced photodecomposition of the samples was observed at 25 °C using the 4880-Å exciting line, some of the Raman spectra were recorded at lower temperature to improve the resolution of the spectra.

For the trans isomer of symmetry D_{4h} a total of 11 fundamentals are expected. These are classified as $2A_{1g} + 2A_{2u} + B_{1g} + B_{2g} + B_{2u} + E_g + 3E_u$. Since the ion has a center of symmetry, the infrared-active bands should be inactive in the Raman spectrum, and vice versa. The B_{2u} mode should be inactive in both the infrared and the Raman spectra. Consequently, we would expect five infrared-active and five Raman-active fundamentals following the principle of mutual exclusion. Of the five Raman-active fundamentals, two should be polarized.

For the cis isomer of symmetry C_{2v} a total of 15 fundamentals are expected which are classified as $6A_1 + 2A_2 + 4B_1 + 3B_2$. Of these, the A_1, B_1, and B_2 modes (total of 13) should be infrared active. All 15 fundamentals should be Raman active and 6 of these should be polarized.

As can be seen from Figure 3 and Table II a total of 10 fundamentals were observed, if we ignore the splittings caused by Fermi resonance (see below). Of these, five are infrared and five are Raman active, and they are mutually exclusive.

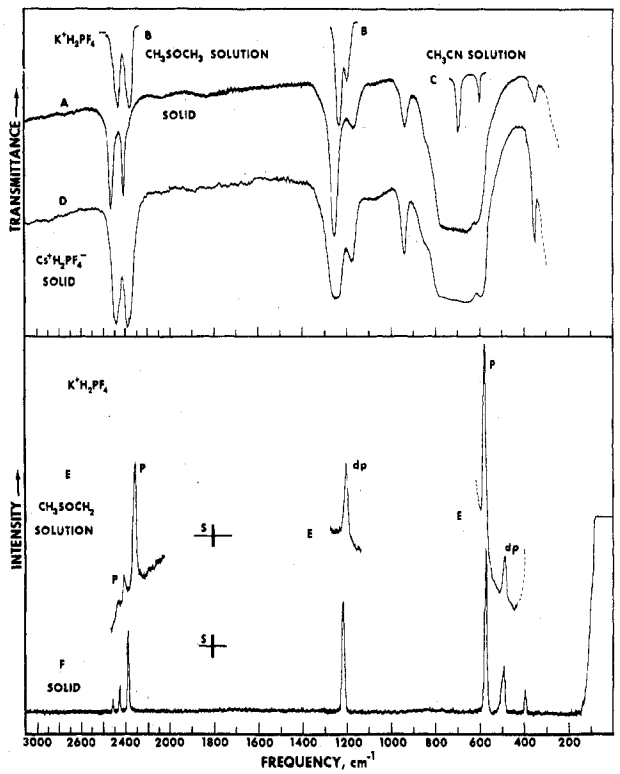

Figure 3. Vibrational spectra of KH_2PF_4 as AgCl disk; the dashed line indicates absorption caused by the window material: traces B and C, solution spectra; trace D, infrared spectrum of solid CsH_2PF_4; trace E, Raman spectrum of KH_2PF_4 in CH_3SOCH_3 solution; p, dp, and S indicate polarized and depolarized bands and spectral slit width, respectively; trace F, Raman spectrum of solid KH_2PF_4 recorded at −90 °C.

Table II. Vibrational Spectra of KH_2PF_4 and CsH_2PF_4 and Their Assignment

Obsd freq, cm^{-1}, and intens[a]								
KH_2PF_4				CsH_2PF_4				
Ir		Raman		Ir	Raman			
Solid	$(CH_3)_2SO$ soln	Solid	$(CH_3)_2SO$ soln	Solid	Solid	$(CH_3)_2SO$ soln	Assignment in point group, D_{4h}	Approx description of vib
2518 s, 2410 s [b]	2467 s, 2360 s [b]			2495 s, 2380 s [b]			$\nu_3(A_{2u})$, $\nu_8 + \nu_9(A_{1u} + A_{2u} + B_{1u} + B_{2u})$	Antisym PH_2 str
		2517 (0.7)	2469 (0.4) p		2505 (0.9)	2470	$2\nu_9(A_{1g} + A_{2g} + B_{1g} + B_{2g})$	
		2453 (1.5)	2418 (1.0) p		2440 (1.5)	2416 (1)	$2\nu_8(A_{1g} + A_{2g} + B_{1g} + B_{2g})$	
		2377 (4.9)	2319 (6.0) p		2341 (5.1)	2319 (6) p	$\nu_1(A_{1g})$	Sym PH_2 str
1253 s, 1171 m [b]	1236 s, 1202 m [b]			1251 s, 1178 m [b]			$\nu_9(E_u)$, $\nu_5 + \nu_{10}(E_u)$	δ sciss PH_2
		1217 (6.7)	1204 (4.0) dp		1212 (5.9)	1206 (4) dp	$\nu_8(E_g)$	δ wag PH_2
937 m				939 m			$\nu_2 + \nu_{11}(E_u)$	
840 sh				845 sh			$\nu_5 + \nu_{11}(E_u)$	
700 vs, br	701 vs[c,d]			700 vs, br			$\nu_{10}(E_u)$	Antisym PF_4 str
608 s	609 s[d]			610 s			$\nu_4(A_{2u})$	δ umbrella PF_4
		575 (10)	582 (10) p		576 (10)	582 (10) p	$\nu_2(A_{1g})$	Sym in-phase PF_4 str
		495 (2.8)	495 (2.1) dp		496 (2.6)	496 (2) dp	$\nu_5(B_{1g})$	Sym out-of-phase PF_4 str
		394 (1.4)	c		397 (1.6)		$\nu_6(B_{2g})$	δ sym in-plane PF_4
355 m				355 m			$\nu_{11}(E_u)$	δ antisym in-plane PF_4

[a] Uncorrected Raman intensities. [b] Braces indicate Fermi resonance. [c] Band obscured by solvent band. [d] Recorded for CH_3CN solution.

Table III. Vibrational Frequencies (cm^{-1}) of the Modes Involving the Square-Planar PF_4 Part of $H_2PF_4^-$ Compared to Those of Similar Molecules and Ions

Approx description of XF_4 mode	PF_6^- [a]	SF_5O^- [b]	$H_2PF_4^-$	ClF_5 [c]	SF_5^- [c]	ClF_4^- [d]	ClF_4O^- [e]
Antisym str	840	785	701	732	590	590	578
Sym in-phase str	735	697	582	538	522	505	456
Sym out-of-phase str	563	541	495	480	435	417	345
Umbrella def	555	506	609	495	466	425	339
Sym in-plane def	462	452	394	375	342	288	283
Antisym in-plane def		325	355	296	241		204

[a] Reference 17. [b] Reference 16. [c] Reference 15. [d] Reference 18. [e] Reference 19.

Furthermore, two of the observed Raman bands are polarized. These data convincingly show that $H_2PF_4^-$ possesses symmetry D_{4h}.

The assignments for $H_2PF_4^-$ (see Table II) were made on the following basis. The two polarized Raman bands must represent the A_{1g} modes with the higher frequency one being the symmetric PH_2 and the lower frequency one being the symmetric in-phase PF_4 stretch. The observation of three Raman bands in the region of the symmetric PH_2 stretch can readily be explained by Fermi resonance between this mode and the combination bands $2\nu_8$ and $2\nu_9$.

The remaining three Raman bands are due to the PH_2 wag, the symmetric out-of-phase PF_4 stretch, and the symmetric in-plane PF_4 deformation, respectively. Their frequencies should decrease in this order and, therefore, their assignment is straightforward.

Of the five infrared-active bands, the antisymmetric PH_2 stretch should have the highest frequency and is assigned to the bands in the 2400-cm^{-1} region. The observed splitting into two bands is caused by Fermi resonance with the combination band $\nu_1 + \nu_9$. The PH_2 scissoring mode should occur at a significantly higher frequency than those of the PF_4 group modes and, hence, is assigned to the strong band at about 1210 cm^{-1}. Again, a splitting is observed owing to Fermi resonance with $\nu_5 + \nu_{10}$.

The remaining three infrared-active modes are the antisymmetric PF_4 stretch, the umbrella PF_4 deformation, and the antisymmetric in-plane PF_4 deformation. The frequencies and the relative intensities of these three fundamentals should decrease in this order. The observed bands are in excellent agreement with these predictions and allow their unambiguous assignment.

In the infrared spectra of the solids the antisymmetric PF_4 stretch results in an extremely broad band, a feature characteristic[8-12] for many square-planar XF_4 groups. In order accurately to locate the band center and to confirm the presence of a single fundamental in this frequency region, solution spectra were recorded. As shown by insert C of Figure 3, the solution spectrum shows a single sharp band at 701 cm^{-1}. The solution spectra also confirm that the splittings observed for the solids for several bands are due to Fermi resonance and are not caused by solid-state effects, since they are also present in the solution spectra. Whereas the solid-state spectra show no significant deviations from the selection rules for point group D_{4h}, significant frequency shifts were observed for several bands on going from the solid state to the solutions. These shifts were most pronounced for fundamentals involving the PH_2 group. Furthermore, the frequency separation of some of the Fermi resonance components in the solution spectra significantly differs from those observed for the solid, thus allowing a somewhat better estimate of the unperturbed frequencies.

Comparison of the frequencies of the modes involving the square-planar PF_4 part of $H_2PF_4^-$ with those of similar square-planar XF_4 groups in related molecules and ions (see Table III),[15-19] shows excellent agreement. The observed frequency trends are as expected for the in-plane modes and confirm the above assignments. The somewhat high-frequency value of the PF_4 umbrella deformation in $H_2PF_4^-$ may be caused by the two axial hydrogen ligands. Since no similar compounds are known, it is impossible to judge whether this frequency increase for the umbrella deformation is characteristic for H_2XF_4 species or not. The frequencies of the PH_2 modes are similar to those observed for other PH compounds, such as PH_3, PH_4^+,[10] H_2PF_3, and HPF_4.[20]

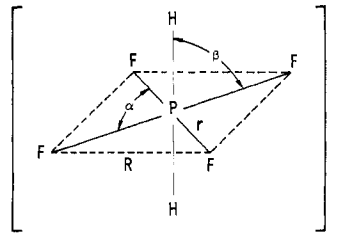

Figure 4. Definition of structural parameters of $H_2PF_4^-$.

Table IV. Symmetry Coordinates[a] for $H_2PF_4^-$

A_{1g}	S_1	$(1/2^{1/2})(\Delta R_1 + \Delta R_2)$
	S_2	$(1/2)(\Delta r_1 + \Delta r_2 + \Delta r_3 + \Delta r_4)$
	S_{r1}	$(1/2)(\Delta\alpha_1 + \Delta\alpha_2 + \Delta\alpha_3 + \Delta\alpha_4)$
	S_{r2}	$(1/8^{1/2})(\Delta\beta_1 + \Delta\beta_2 + \Delta\beta_3 + \Delta\beta_4 + \Delta\beta_5 + \Delta\beta_6 + \Delta\beta_7 + \Delta\beta_8)$
A_{2u}	S_3	$(1/2^{1/2})(\Delta R_1 - \Delta R_2)$
	S_4	$(1/8^{1/2})(\Delta\beta_1 + \Delta\beta_2 + \Delta\beta_3 + \Delta\beta_4 - \Delta\beta_5 - \Delta\beta_6 - \Delta\beta_7 - \Delta\beta_8)$
B_{1g}	S_5	$(1/2)(\Delta r_1 - \Delta r_2 + \Delta r_3 + \Delta r_4)$
	S_{r5}	$(1/8^{1/2})(\Delta\beta_1 - \Delta\beta_2 + \Delta\beta_3 - \Delta\beta_4 + \Delta\beta_5 - \Delta\beta_6 + \Delta\beta_7 - \Delta\beta_8)$
B_{2g}	S_6	$(1/2)(\Delta\alpha_1 - \Delta\alpha_2 + \Delta\alpha_3 - \Delta\alpha_4)$
B_{2u}	S_7	$(1/8^{1/2})(\Delta\beta_1 - \Delta\beta_2 + \Delta\beta_3 - \Delta\beta_4 - \Delta\beta_5 + \Delta\beta_6 - \Delta\beta_7 + \Delta\beta_8)$
E_g	S^x_8	$(1/2)(\Delta\beta_1 - \Delta\beta_3 + \Delta\beta_5 - \Delta\beta_7)$
	S^y_8	$(1/2)(\Delta\beta_2 - \Delta\beta_4 + \Delta\beta_6 - \Delta\beta_8)$
E_u	S^x_9	$(1/2)(\Delta\beta_1 - \Delta\beta_3 + \Delta\beta_5 - \Delta\beta_7)$
	S^x_{10}	$(1/2^{1/2})(\Delta r_1 - \Delta r_3)$
	S^x_{11}	$(1/2)(\Delta\alpha_1 - \Delta\alpha_2 - \Delta\alpha_3 + \Delta\alpha_4)$
	S^y_9	$(1/2)(\Delta\beta_2 - \Delta\beta_4 + \Delta\beta_6 - \Delta\beta_8)$
	S^y_{10}	$(1/2^{1/2})(\Delta r_2 - \Delta r_4)$
	S^y_{11}	$(1/2)(\Delta\alpha_1 + \Delta\alpha_2 - \Delta\alpha_3 - \Delta\alpha_4)$

[a] S_{r1}, S_{r2}, and S_{r5} are the redundant coordinates.

Normal-Coordinate Analysis. A normal-coordinate analysis of $H_2PF_4^-$ was carried out. The definition of the structural parameters is shown in Figure 4. The bond lengths were estimated to be $r(PF) = 1.60$ Å and $R(PH) = 1.40$ Å by comparison with similar molecules and ions. All bond angles were assumed to be 90° as required for D_{4h}. The symmetry coordinates used for $H_2PF_4^-$ are given in Table IV. The **G** matrix and Z transformation were evaluated numerically.[21] The correctness of this transformation was verified by showing that the **G** matrix and Z transformation were the direct sum of each symmetry block and that the frequencies computed ignoring symmetry were the same after the symmetry transformation was made. Only those **F** matrix elements regarded as more important were considered and the analytical **F** matrix is shown in Table V. For the computation of the force constants, the frequency values of the free $H_2PF_4^-$ ion,

Table V. Observed Frequencies (cm^{-1}), Symmetry, Some Internal Force Constants,[a,b] and Potential Energy Distribution[c] of $H_2PF_4^-$

		Freq			F		PED	
					$F_{11,11} \equiv$ Min	$F_{10,11} \equiv$ 0	$F_{11,11} \equiv 0$	$F_{10,11} \equiv 0$
A_{1g}	ν_1	2322	F_{11}	$f_R + f_{RR}$		3.201		$100F_{11}$
	ν_2	582	F_{22}	$f_r + 2f_{rr} + f_{rr}'$		3.790		$100F_{22}$
A_{2u}	ν_3	2390	F_{33}	$f_R - f_{RR}$		3.174		$100F_{33}$
	ν_4	609	F_{44}	$f_\beta + f_{\beta\beta} - f_{\beta\beta'} + 2f_{\beta\beta''} - f_{\beta\beta'''} - 2f_{\beta\beta''''}$		1.615		$100F_{44}$
B_{1g}	ν_5	495	F_{55}	$f_r - 2f_{rr} + f_{rr}'$		2.742		
B_{2g}	ν_6	394	F_{66}	$f_\alpha - 2f_{\alpha\alpha} + f_{\alpha\alpha'}$		1.112		
B_{2u}	ν_7		F_{77}	$f_\beta + f_{\beta\beta} - f_{\beta\beta'} - 2f_{\beta\beta''} - f_{\beta\beta'''} + 2f_{\beta\beta''''}$				
E_g	ν_8	1205	F_{88}	$f_\beta - f_{\beta\beta} - f_{\beta\beta'} + f_{\beta\beta'''}$		0.812		
E_u	ν_9	1232	F_{99}	$f_\beta - f_{\beta\beta} + f_{\beta\beta'}$	0.814			$97F_{99}$
	ν_{10}	701	$F_{10,10}$	$f_r - f_{rr'}$	2.864	2.153	$107F_{10,10} - 19F_{10,11} + 9F_{11,11}$	$74F_{10,10} + 23F_{11,11}$
	ν_{11}	355	$F_{11,11}$	$f_\alpha - f_{\alpha\alpha'}$	1.176	1.430	$100F_{11,11}$	$23F_{10,10} + 77F_{11,11}$
			$F_{10,11}$	$2^{1/2}f_{r\alpha}$	0.560	0		
			f_R			3.188		
			f_{RR}			0.014		
			f_r		3.065	2.710		
			f_{rr}			0.262		
			$f_{rr'}$		0.201	0.557		

[a] Stretching constants in mdyn/Å, deformation constants in mdyn Å/radian^2, and stretch-bend interaction constants in mdyn/radian. [b] f_{rr} and $f_{rr'}$ are the interactions between perpendicular and collinear PF bonds, respectively; $f_{\alpha\alpha}$ and $f_{\alpha\alpha'}$ are the interactions between angles having a common and no common fluorine atom, respectively; $f_{\beta\beta}$, $f_{\beta\beta'}$, $f_{\beta\beta''}$, $f_{\beta\beta'''}$, and $f_{\beta\beta''''}$ are the interactions between angles being coplanar with a common H, coplanar with a common F, perpendicular with a common H, coplanar without a common atom, and perpendicular without a common atom, respectively; $f_{r\alpha}$ is the interaction between a PF stretch and α having a common F. F matrix elements considered less important were omitted. [c] Contributions of less than 5% are not listed.

i.e., the solution values, were used (see Table V), after applying small frequency corrections to the modes disturbed by Fermi resonance.

The computed force constants are shown in Table V. Whereas the values obtained for the B_{1g}, B_{2g}, and E_g block are unique, the remaining blocks are underdetermined. In the A_{1g} block, the G_{12} element equals zero. Therefore, the F_{12} term can be neglected, and F_{11} and F_{22} should be close approximations to a general valence force field. In the A_{2u} block, we have only one stretching and one deformation vibration of very different frequency. Coupling between these two modes is expected to be small and, hence, F_{34} was assumed to be zero. This choice is supported by the potential energy distribution (see Table V) which shows both fundamentals to be 100% characteristic.

For the remaining E_u block, the interaction term $F_{10,11}$ was found to strongly influence the values of $F_{10,10}$ and $F_{11,11}$. Consequently, we have computed F_{99}, $F_{10,10}$, and $F_{11,11}$ as a function of $F_{10,11}$. The important sections of the resulting force constant ellipses are shown in Figure 5. It has previously been shown[22] that the most probable range for F_{xy} is limited by the extremal values F_{yy} and F_{xy} = minimum. These limits suggest uncertainties of about ±0.2 mdyn/Å for f_r and f_{rr} and of about ±0.1 mdyn/Å for f_α. However, the general valence force field is probably closer to the $F_{10,11}$ = mimimum solution and therefore, values such as f_r = 2.97 ± 0.10 and f_{rr} = 0.36 ± 0.10 mdyn/Å seem more realistic.

A summary of the computed force constants and the potential energy distribution are listed in Table V. As can be seen all fundamentals are highly characteristic. The most interesting internal force constants of $H_2PF_4^-$ are the PF and the PH stretching constants since they are a measure for the relative bond strength of these bonds.

The value of the PH stretching force constant f_R (3.19 mdyn/Å) of $H_2PF_4^-$ is in excellent agreement with those of 3.19 and 3.10 mdyn/Å found[10] for PH_4^+ and PH_3, respectively. This indicates that the PH bonds in $H_2PF_4^-$ are highly covalent with a bond order of approximately 1.

Contrary to the PH bonds, the PF stretching force constant f_r (2.97 mdyn/Å) of $H_2PF_4^-$ has a surprisingly low value when compared to those of 4.39 and 5.21 mdyn/Å previously reported for PF_6^- [23] and PF_3,[17] respectively. The low value of

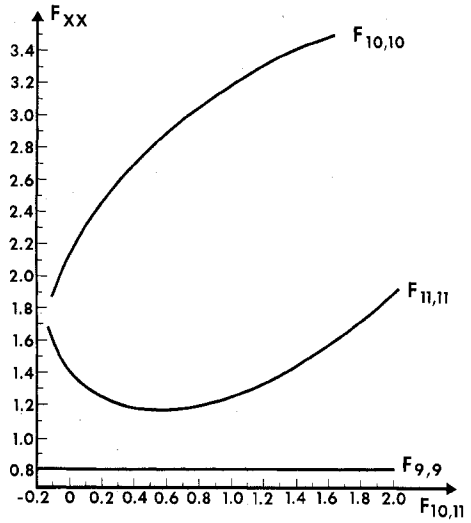

Figure 5. Force constant ellipses for the E_u block of $H_2PF_4^-$. The values of the diagonal symmetry force constants are given as a function of $F_{10,11}$.

f_r in $H_2PF_4^-$ indicates highly polar PF bonds with a bond order closer to 0.5 than to 1. Obviously, the negative charge in $H_2PF_4^-$ resides mainly on the highly electronegative fluorine ligands. A bonding scheme, similar to that previously invoked for the square-planar $HalF_4^-$ anions,[18,24,25] might also be applicable to the square-planar PF_4 part of $H_2PF_4^-$. Both types of anions are structurally closely related. In $HalF_4^-$ the two axial positions are occupied by two free valence electron pairs, whereas in $H_2PF_4^-$ they are occupied by two hydrogen ligands which readily release electron density to the PF_4 part of the anion.

General Considerations. The limited number of known examples of pseudooctahedral AF_4X_2 species indicates that the nature of the X ligand determines which stereoisomer is preferred. If X is a free valence electron pair[18,24-26] or a group of low electronegativity, such as H or CH_3,[2] the trans isomer is preferred, but if X is multiply bonded oxygen,[7,11] the cis isomer is preferred. If X is of intermediate electronegativity, such as OH, OCH_3, Cl, Br, etc.,[9,11-14] both the cis and the

trans isomers have been observed. An attempt will be made to rationalize these observations.

For X being a free-valence electron pair, the preference for the trans isomer can be explained by the fact the two free-valence electron pairs seek high s character,[27] i.e., form a linear sp hybrid. This results in strong contributions from semiionic three center-four electron bonds[28-30] to the AF_4 part. Since the 3c–4e bonds involve a single p orbital of the central atom for the bonding of two F ligands, the resulting F–A–F group must possess an approximately linear configuration. Since a linear X–A–X and two linear F–A–F groups are possible only for the trans isomer, this should be the preferred configuration.

The trans configuration of $H_2PF_4^-$ can be rationalized by both the 3c–4e bond model and intramolecular attractive forces between the H and the F ligands. The latter rationale is based on the assumption that the negatively polarized fluorine ligands are attracted by the positively polarized hydrogen ligands. In the trans isomer, each H possesses four closest F neighbors, and each F has two closest H neighbors. In the cis isomer, however, each H possesses only three closest F neighbors, and two of the fluorines possess only one closest H neighbor. Therefore, the trans isomer is expected to be energetically favored over the cis isomer.

If X is oxygen, the more electronegative fluorine ligands tend to polarize the X–O bonds. This results in an increased bond order of the X–O bonds according to

$$^{-}:\ddot{O}-X-F \leftrightarrow :\dot{O}=X\ F^{-}$$

and

$$:\dot{O}=X-F \leftrightarrow {}^{+}:O\equiv X\ F^{-}$$

and allows the shifting of a formal negative charge from the less electronegative oxygen ligand to the more electronegative fluorine ligand. Molecular orbital following arguments favor this kind of resonance for linear F–A–O groups. However, these are only possible for the cis isomer.

For singly bonded ligands of intermediate electronegativity, such as OH, OCH_3, Cl, Br, etc., both cis and trans isomers have been observed.[9,11-14] This indicates that other factors, such as steric effects or the nature of the formation reaction mechanism, become more important. Consequently, predictions of the expected stereoisomer will be considerably more difficult for these ligands.

Acknowledgment. We are grateful to Dr. L. R. Grant for helpful discussions and to the Office of Naval Research, Power Branch, for financial support.

Registry No. KF, 7789-23-3; CsF, 13400-13-0; H_2PF_3, 13659-65-9; KH_2PF_4, 58188-50-4; CsH_2PF_4, 58188-51-5.

References and Notes

(1) R. R. Holmes and R. N. Storey, *Inorg. Chem.*, **5**, 2146 (1966).
(2) R. Schmutzler, *Adv. Fluorine Chem.*, **5**, 31 (1965); W. Stadelmann, O. Stelzer, and R. Schmutzler, *Z. Anorg. Allg. Chem.*, **385**, 142 (1971).
(3) S. S. Chan and C. J. Willis, *Can. J. Chem.*, **46**, 1237 (1968).
(4) E. K. Plyler, A. Danti, L. R. Blaine, and E. D. Tidwell, *J. Res. Natl. Bur. Stand.*, **64**, 841 (1960).
(5) H. H. Claassen, H. Selig, and J. Shamir, *Appl. Spectrosc.*, **23**, 8 (1969).
(6) F. A. Miller and B. M. Harney, *Appl. Spectrosc.*, **24**, 291 (1970).
(7) A. Engelbrecht, O. Mayr, G. Ziller, and E. Schandara, *Monatsh. Chem.*, **105**, 796 (1974).
(8) H. A. Carter, J. N. Ruddick, J. R. Sams, and F. Aubke, *Inorg. Nucl. Chem. Lett.*, **11**, 29 (1975).
(9) A. Clouston, R. D. Peacock, and G. W. Fraser, *Chem. Commun.*, 1197 (1970).
(10) K. Seppelt, *Z. Anorg. Allg. Chem.*, **406**, 287 (1974).
(11) G. W. Fraser and G. D. Meikle, *J. Chem. Soc., Chem. Commun.*, 624 (1974).
(12) U. Elgad and H. Selig, *Inorg. Chem.*, **14**, 140 (1975).
(13) I. Agranat, M. Rabinovitz, and H. Selig, *Inorg. Nucl. Chem. Lett.*, **11**, 185 (1975).
(14) Yu. A. Buslaev and E. G. Ilyin, *J. Fluorine Chem.*, **4**, 271 (1974).
(15) K. O. Christe, E. C. Curtis, C. J. Schack, and D. Pilipovich, *Inorg. Chem.*, **11**, 1679 (1972).
(16) K. O. Christe, C. J. Schack, D. Pilipovich, E. C. Curtis, and W. Sawodny, *Inorg. Chem.*, **12**, 620 (1973).
(17) H. Siebert, "Anwendungen der Schwingungsspektroskopie in der Anorganischen Chemie", Springer Verlag, Berlin (1966).
(18) K. O. Christe and W. Sawodny, *Z. Anorg. Allg. Chem.*, **374**, 306 (1970).
(19) K. O. Christe and E. C. Curtis, *Inorg. Chem.*, **11**, 2209 (1972).
(20) R. R. Holmes and C. J. Hora, Jr., *Inorg. Chem.*, **11**, 2506 (1972).
(21) E. C. Curtis, Report R-6768, Rocketdyne, Canoga Park, Calif., Oct 1966.
(22) W. Sawodny, *J. Mol. Spectrosc.*, **30**, 56 (1969).
(23) K. O. Christe and R. D. Wilson, *Inorg. Chem.*, **14**, 694 (1975).
(24) K. O. Christe and C. J. Schack, *Inorg. Chem.*, **9**, 1852 (1970).
(25) K. O. Christe and D. Naumann, *Inorg. Chem.*, **12**, 59 (1973).
(26) J. G. Malm, H. Selig, J. Jortner, and S. A. Rice, *Chem. Rev.*, **65**, 199 (1965).
(27) K. O. Christe, *Proc. Int. Congr. Pure Appl. Chem.*, **24**, No. 4, 115 (1974).
(28) G. C. Pimentel, *J. Chem. Phys.*, **19**, 446 (1951).
(29) R. J. Hach and R. E. Rundle, *J. Am. Chem. Soc.*, **73**, 4321 (1951).
(30) R. E. Rundle, *J. Am. Chem. Soc.*, **85**, 112 (1963).

Contribution from the Department of Chemistry, University of Pennsylvania, Philadelphia, Pennsylvania 19174

Silylphosphonium Compounds. Synthesis and Structure

H. SCHÄFER* and A. G. MacDIARMID

Received October 20, 1975 AIC50752W

Trimethylsilylcobalt tetracarbonyl, $Me_3SiCo(CO)_4$, has been found to react instantly with Me_3P, Me_2PSiMe_3, and $MeP(SiMe_3)_2$ to give the solid silylphosphonium compounds $[Me_3SiPMe_3]^+[Co(CO)_4]^-$, $[(Me_3Si)_2PMe_2]^+[Co(CO)_4]^-$, and $[(Me_3Si)_3PMe]^+[Co(CO)_4]^-$, respectively, each of which contain at least one Si–P bond. No reaction occurs with $(Me_3Si)_3P$. The infrared and Raman spectra of the compounds are completely consistent with the phosphonium salt formulation. A single-crystal x-ray study of $[(Me_3Si)_2PMe_2]^+[Co(CO)_4]^-$ shows that the bonding at both the phosphorus and cobalt atoms is almost exactly tetrahedral. A concentration- and temperature-dependent NMR study shows that the compounds dissociate in solution to $Me_3SiCo(CO)_4$ and the phosphine and that the dissociation increases with (i) the number of Me_3Si groups in the cation, (ii) increasing temperature, and (iii) decreasing concentration.

Introduction

In a preliminary study[1,2] we had reported a new type of reaction between a transition metal carbonyl and a phosphine. It was found that Me_3P did not react with $Me_3SiCo(CO)_4$ in the expected manner to form $Me_3SiCo(CO)_3PMe_3$. Instead, an instantaneous reaction occurred to give quantitative yields of the solid silylphosphonium compound $[Me_3SiPMe_3]^+[Co(CO)_4]^-$, the first reported example of a phosphonium compound containing an Si–P bond. Detailed studies of the

* To whom correspondence should be addressed at the Institut für Anorganische Chemie der Universität, 75 Karlsruhe, West Germany.